

Simulating the Dissolution and Growth of Zeolite Beta C**

May E. Chiu, Ben Slater,* and Julian D. Gale

Understanding how zeolites form on the atomic scale, under natural or laboratory conditions, remains a fundamental challenge to both experiment and theory. One goal of these studies is to control and manipulate the mechanism and rate of formation to produce tailored nanoporous materials whose unique framework architectures and voids provide channels or cages with exceptional reactive environments and sieving capabilities.^[1] One of the most enduring questions, despite many decades of very active research, concerns the role of primary building units (PBUs, that is, silicate monomers) and secondary building units (SBUs, that is, polymeric or oligomeric silicates) in the crystal-growth mechanism. For example, whereas NMR spectroscopy has been used extensively to identify units present in the mother liquor, the precise configurations, charge state, proportion of monomers to dimers and higher oligomers, and the role of these units within crystal growth remain controversial subjects.^[2–4] There is a clear need to determine the extent to which primary and secondary building units influence the mechanism and rate of growth, and the focus of the work described herein is to investigate layer assembly by monomers through atomistic computer-simulation techniques. We now relate how the dissolution and growth processes can be studied simultaneously and consider the implications of our results for monomer-mediated and monomer-with-oligomer growth.

Our model system to investigate growth and dissolution is zeolite beta C, a recently synthesized^[5] member of the zeolite beta family, first predicted by Treacy, Newsam, and co-workers,^[6] which exhibits a 3D interpenetrating 12-membered ring (MR) network. In previous work^[7] we examined the surface structure of the (100) face of zeolite beta C to rationalize observations from HREM measurement. Figure 1 shows the framework structure of zeolite beta C; only the

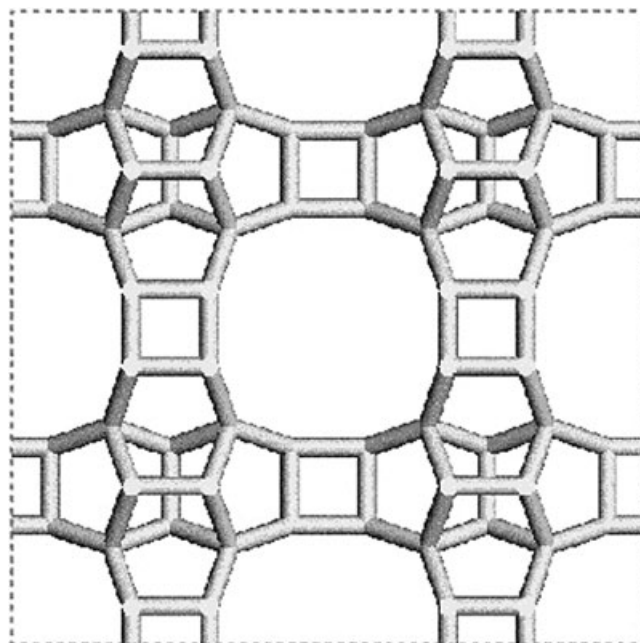


Figure 1. The unit cell and silicon-only framework of zeolite beta C viewed along [100]. Vertices indicate silicon atoms.

silicon atoms are shown, and the central 12-MR channel can be seen clearly in the center of the figure. We previously showed that two terminations imaged with HREM^[7] (Figure 2 a, b, and c), could be explained by first-principle results. In particular, the absence of the surface structure (Figure 2 e and h), which classical calculations predict to have equal stability to structures shown in Figure 2 d and f (and g and i), can be rationalized through the formation of single- and double- 4-rings and their subsequent reaction with the crystal surface. These calculations support the view that SBUs can play a part in the assembly of framework materials, but they pertain to a very small component of the growth process. It has been found that characteristic terminations are observed on crystal surfaces that correspond to thermodynamic minima; these surface architectures are long-lived states during the crystal-growth process, and hence intermediary structures are, by implication, relatively short-lived or not extant at any stage of the crystal layer assembly. Herein, we study the intermediate stages of growth and determine whether exotic terminating structures have similar stabilities (thermodynamically accessible) to those observed experimentally. We also assess whether the growth could be mediated by PBUs or SBUs.

Owing to the unit-cell size and density, coupled with the vast number of unique and hypothetical terminating surface structures that can be imagined, we were compelled to use the Born model of solids, which employs shell-model interionic potentials^[8] to model the crystal bulk and surface structure, in order to decrease simulation expense. All calculations were carried out with GULP3.0^[9] code to relax both bulk and surface configurations. Terminating silanol species are represented by two- and three-body potentials.^[10] Additionally, the surface energy is corrected for the presence of a solvent continuum through the newly implemented algorithm

[*] M. E. Chiu
Department of Chemistry, University of Cambridge
Lensfield Road, Cambridge, CB2 1EW (UK)

Dr. B. Slater
The Davy–Faraday Research Laboratory
The Royal Institution of Great Britain
21 Albemarle Street, London, W1S 4BS (UK)
Fax: (+44) 20-729-3569
E-mail: ben@ri.ac.uk

J. D. Gale
Nanochemistry Research Institute
Department of Applied Chemistry
Curtin University of Technology
P.O. Box U1987, Perth 6845 (Australia)

[**] B.S. would like to thank the Nuffield Foundation for providing a student bursary for M.C. J.D.G. acknowledges the support of the Government of Western Australia through a Premier's Research Fellowship.

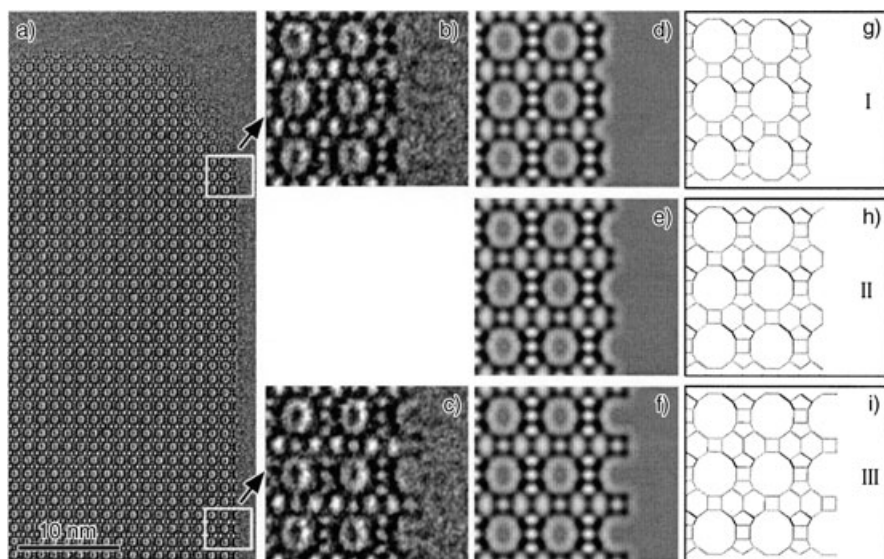


Figure 2. Comparison of high-resolution electron microscopy (HREM) and simulation results taken from Slater et al.^[7] Parts a), b), and c) are HREM images; g), h), and i) are simulation predictions. Parts d), e), and f) are simulated HREM patterns based on structure predictions g), h), and i), respectively.

COSMIC,^[11] which adapts the widely used COSMO^[12] approach for the treatment of 2D periodic surfaces. In this case, the solvation energy is determined based on a single-point calculation taking the dielectric constant of water to be 78.4. To model the crystal surface, a semi-infinite approach is used which is equivalent to the theoretical approach used in previous work.^[7] The model of the crystal surface is constructed with four layers of zeolite beta C, divided into an upper region (containing two layers) that is fully relaxed and a lower region (containing two layers), which is held fixed to represent the long-range potential of the underlying bulk material.

To survey the structures that can be sampled during growth, it is simpler to mimic a dissolution process rather than growth, so that possible geometries are revealed as each unit is removed. The structure shown in Figure 2h is used as the starting point for a hypothetical dissolution reaction. Note that the starting point is not important for structure generation as the purpose of the experiment is to generate “hypothetical” structures. Hence, there is no *deterministic* factor that controls which structures are sampled. A single-crystal-growth layer containing 32 silicon tetrahedra (equivalent to the number of formula units within the unit cell) is removed systematically by “dissolving” one silicon tetrahedron (T site) after another until the original starting configuration is regenerated. At each step, one silicon atom is selected from one of the symmetry-inequivalent surface-accessible sites. (Such sites are those that would be in contact with the solvent. In total, over 130 unique configurations were considered; in some instances, owing to fourfold symmetry equivalence, only one configuration needs to be considered for each step, but in the latter stages of the dissolution/growth model, up to 11 symmetrically distinct silicon atoms are exposed at the surface and hence 11 surface structures are

relaxed.) The accessibility of the surface sites is actually determined crudely with a search radius of 2.5 Å below the uppermost silicon site. Two of the four oxygen atoms bonded to the silicon are then selected and a charge-neutral SiO₂ fragment is displaced to the bottom of the upper (relaxed) layer. The corresponding symmetry-related fragment within the upper layer is displaced to the base of the lower (fixed) layer. This operation guarantees that the number of species within the lower region remains the same throughout the simulation, so that the surface energy and electrostatics are well-behaved. It also ensures that the newly created surface is nonpolar. Herein, we have restricted the study to monomeric units to decrease the configurational permutations to a computable quantity.

It is presumed that under typical hydrothermal synthesis conditions, the coordinatively unsaturated fragment and surface react with water, which heterolytically splits to form proton and hydroxide species that bind to the undercoordinated oxygen and silicon sites, respectively, such that no undercoordinated

sites are exposed on any of the intermediate structures that are generated. A charge-neutral fragment (SiO₂) would be expected to react with water to form dispersed PBUs (Si(OH)₄), which would be absorbed in a sol-gel layer above the hydroxylated surface. However, this contribution is not explicitly included in the model described herein. Driver software was developed to effect the stepwise displacement of neutral SiO₂ units which also reconstructs and hydroxylates surface structures to generate nonpolar surface terminations. The Helmholtz surface energy^[13] is calculated at each stage to evaluate surface stability. This calculation includes the energy required to dissociate water at the surface, to ensure that the surface energy describes the total work done per unit area in a closed Born–Haber cycle. The latter procedure has been used extensively,^[13, 14] and is described in detail in the report of Parker and co-workers.^[15]

Figure 3a describes the surface energy as a function of the number of T sites removed. Only the lowest-energy configuration is reported, and hence the configurations are notionally indicative of a minimum-energy pathway for dissolution or growth. As the crystal surface is dissolved, the surface becomes more enthalpically unstable until approximately 3/4 of a surface layer is dissolved; thereafter, dissolution is exothermic. The process of dissolution can be interpreted from a converse perspective, reading the graph from right to left, whereby the *growth* by monomer addition is described. The dissolution process is initially endothermic, and thereafter exothermic, which is qualitatively consistent with experimental observations.

The first point on the graph corresponds to the terminating structure given in Figure 2e or 2h. Interpreting the graph from left to right, it can be observed that the surface energy rises slightly for the first two T sites removed, rises sharply as a third site is removed, and finally drops to an energy

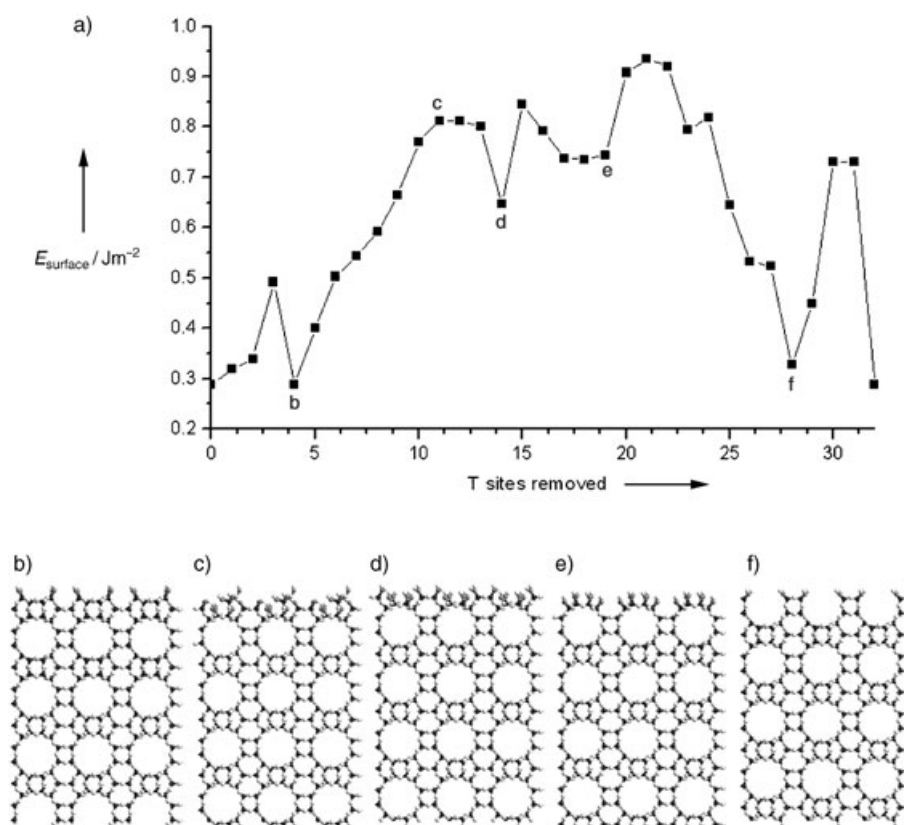


Figure 3. a) Surface energy as a function of the number of T sites removed with selected surface configurations. b)–f) Depictions of selected points along the minimum surface energy pathway, as indicated on the graph in part a). Silicon atoms are shown in black, lattice oxygen atoms in gray, hydrogen in white, and hydroxy oxygen atoms in dark gray. The surface shown is the (100) surface in cross section through the [100] axis. The top of each cross section represents the crystal terminating structure.

comparable with that of the starting structure. This process relates to the stepwise dissolution of a 4-ring expressed at the crystal surface. Removing the first two sites creates silicon sites with geminal hydroxy functions, whilst loss of the third T site creates a very unstable Si site bonded to three hydroxy groups (a trimeric species). Subsequent removal of T sites results in a general monotonic increase in the surface energy, accompanied by a rise in the density of silanol groups per unit area. Steps 11–13 are almost equivalent in energy, as are steps 17–19, suggesting that growth and dissolution occur with similar rates. After step 21, the general trend is for the surface energy to decrease rapidly, accompanied by a release of energy. Figure 3b–f illustrates five structures, selected from different regions of the dissolution process. Figure 3b shows a surface that is equivalent to that observed in HREM (Figure 2). Figure 3c shows a partially dissolved layer that is composed of 4- and 5-rings (common to beta and, for example, Mordenite zeolites) and a high density of intramolecular hydrogen-bonded silanol groups. Figure 3d shows a local minimum in the surface energy, in which the structure has been dissolved further to create a relatively atomically smooth surface. This can be further dissolved, with an energetic penalty, to the state shown in Figure 3e in which

the 12-MR channel system lies directly below the surface, protected by a very thin membrane of siliceous material. When this membrane is dissolved there is a substantial increase in energy, but subsequent dissolution is relatively facile and exothermic. The final structure formed (Figure 3f) is equivalent to that shown in Figure 2c,f, and i, and has an energy almost equivalent to those of the structures observed at steps 0 and 4 of Figure 3a. There are three global minima, and hence this exhaustive survey corroborates earlier assertions that terminations observed by microscopy techniques correspond to surface-energy minima. Notably, the most endothermic steps are those associated with the interruption of channels or cages (such as the 12-MR) or the formation of highly unstable species with three silanol groups bonded to a single silicon site.

By examining the growth process (Figure 3a right to left), it is clear that there is a substantial energetic penalty associated with the formation of a closed 12-MR channel—a process of clathration around the solvent/sol-gel mixture. However, once this barrier is overcome, the general trend is for the surface to become more stable, with

large decreases in surface energy that are associated with formation of closed loops, such as ring systems or channels.

A more detailed display of the energy changes (Figure 4) shows the net change in energy associated with removing (or in a contrary sense, adding) a T site from the surface. The energy changes are calculated *with respect to the previous step* and include corrections for the solvation energy. It is clear that the dissolution consists of mainly endothermic steps that have a maximum absolute energy of ≈ 2.9 eV. Reading the figure from right to left to interpret growth (taking into account that the 31st step is the first step of growth), again it can be seen that maximum endothermic energy change associated with stepwise growth is up to ≈ 2.9 eV. Note that the maxima associated with endothermic changes occur as isolated peaks and are accompanied by satellite exothermic troughs in the surface energy. One interpretation of these data is that these relatively unfavorable steps during growth (or dissolution) could be avoided if cooperative events, such as the dissolution or addition of dimeric (or higher-order oligomeric) species, occurred. The precise mechanism and rate-determining step of growth/dissolution would therefore be highly dependent on the distribution and population of oligomers within solution. Furthermore, it is well known from

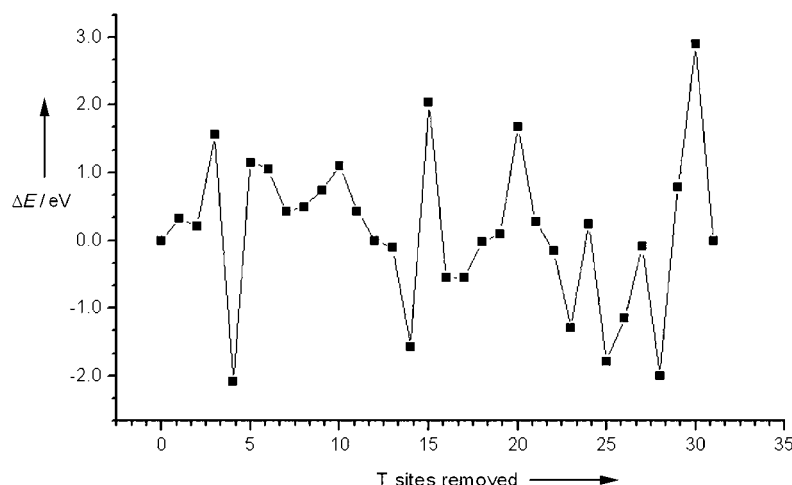


Figure 4. Change in energy for contiguous dissolution with respect to each previous step.

experiment that the distribution of oligomers is highly influenced by the pH value of the solution. Consequently, the role of oligomers in facilitating crystal growth may be a function of pH. A further complication is that the pH value rises during synthesis, a phenomenon that would tend to dissolve small unstable oligomeric species, thus creating more highly charged monomeric species. This suggests that at different stages of growth, crystal assembly may involve distinct species from those involved at lower pH values.

The maximum absolute enthalpy change of $+2.9 \text{ eV}$ ($\approx 280 \text{ kJ mol}^{-1}$) is clearly very large; however, the majority of enthalpy changes are much less than $+2.0 \text{ eV}$. Notwithstanding the magnitude of enthalpy changes, there are a number of factors missing from our model that would substantially lower the energy barrier for growth/dissolution. The present model for the solvent is an approximation, and needs to be enhanced to describe strong interactions, especially in sterically confined regions. Entropy changes of the solvent that arise from the ordering of water are probably larger than the change in the number of species, and may be of similar magnitude to vibrational entropy changes associated with the condensation of monomers to the surface. The solvation energy calculated for all structures was between 0.3 eV and 0.7 eV , though we expect that the solvation energy would increase upon relaxation, particularly for the least stable surfaces, which express a high density of silanol groups. Further details of the solvation of surfaces and all the structures assessed will be reported in a separate publication. We anticipate that most of these effects will systematically lower the surface energy and probably the energy difference between metastable surfaces as well. Correspondingly, the energy barriers should also be diminished. Almost certainly, of far greater significance to the accuracy of our calculations is the absence of pH effects and the mineralizer (fluoride), both of which will substantially lower the barrier to growth. Typical energy barriers measured for zeolitic materials that are relatively simple to synthesize are in the order of $\approx 0.5\text{--}1.4 \text{ eV}$,^[16–22] which when taken with the observation that beta C is difficult to synthesize, suggest that the energy barrier of $\approx 2.0\text{--}2.9 \text{ eV}$ may not be grossly in

error. However, we assume that the activation barrier associated with the surface and monomer/oligomeric complex is substantially smaller than the monomeric condensation barrier (calculated to be $\approx 0.4\text{--}1.0 \text{ eV}$).^[23] If oligomers alter the course of the minimum energy pathway by eliminating the most endothermic processes, then the barrier becomes close to $\approx 1 \text{ eV}$, in very reasonable agreement with measurements. Recent work by Mora-Fonz et al.^[24] suggests that the condensation enthalpy of two monomers is very low ($\approx -0.1 \text{ eV}$) and that the formation energy becomes more favorable in general as monomers condense onto large solution fragments. The use of this as a discriminator to indicate the upper bound for monomer-mediated growth would imply that only approximately half of the steps are viable, and that the supply of specific oligomers may control a substantial part of crystal assembly.

This work explores the enthalpy changes associated with monomeric growth and dissolution to assess whether there is evidence that growth (in particular) can proceed exclusively by addition of monomers, or whether oligomers are required to build the crystal. The results provide strong evidence that the barriers to growth are sufficiently low that one cannot discount the role of monomeric fragments during growth or dissolution. Our evidence suggests that many and possibly all of the stages of growth are thermally accessible, but oligomers may play a key role in overcoming the least-favorable (i.e., rate-determining) stages of growth. These include the assembly of double 4-rings at the crystal surface (indicated by Figure 4) through concerted condensation, for example, of dimeric or trimeric species with the crystal surface, or by reaction of larger preformed oligomers (such as double 4-rings) with the surface. It is clear that experimental data (e.g. NMR spectroscopy) relating to the distribution of oligomers within solution and their sensitivity to extra-framework cations, pH, and other synthesis parameters are needed before the role of PBUs and SBUs during growth can be definitively assigned. However, it is already known that the contents of solution can be manipulated or skewed, such as in the synthesis of purely siliceous zeolite A (which can be regarded as being made entirely from double 4-ring units), recently reported by Corma et al.,^[25,26] in which the unusually stable double 4-ring is presumed to be in excess of other fragments. Future simulation work will employ FP methods to estimate the barrier heights that govern the type of species that form in solution, at what rate, and the reactions of these species with zeolite surfaces.

Received: August 5, 2004

Published online: January 5, 2005

Keywords: crystal growth · solid-state structures · solvent effects · surface chemistry · zeolites

[1] C. S. Cundy, P. A. Cox, *Chem. Rev.* **2003**, *103*, 663.

[2] C. E. A. Kirschhock, R. Ravishankar, F. Verspeurt, P. J. Grobet, P. A. Jacobs, J. A. Martens, *J. Phys. Chem. B* **1999**, *103*, 4965.

- [3] C. T. G. Knight, S. D. Kinrade, *J. Phys. Chem. B* **2002**, *106*, 3329.
- [4] C. E. A. Kirschhock, R. Ravishankar, F. Verspeurt, P. J. Grobet, P. A. Jacobs, J. A. Martens, *J. Phys. Chem. B* **2002**, *106*, 3333.
- [5] Z. Liu, T. Ohsuna, O. Terasaki, M. A. Camblor, M. J. Diaz-Cabanas, K. Hiraga, *J. Am. Chem. Soc.* **2001**, *123*, 5370.
- [6] J. M. Newsam, M. M. J. Treacy, W. T. Koetsier, C. B. Degruyter, *Proc. R. Soc. London Ser. A* **1988**, *420*, 375.
- [7] B. Slater, C. Richard, A. Catlow, Z. Liu, T. Ohsuna, O. Terasaki, M. A. Camblor, *Angew. Chem.* **2002**, *114*, 1283; *Angew. Chem. Int. Ed.* **2002**, *41*, 1235.
- [8] M. J. Sanders, M. Leslie, C. R. A. Catlow, *J. Chem. Soc. Chem. Commun.* **1984**, 1271.
- [9] J. D. Gale, A. L. Rohl, *Mol. Simul.* **2003**, *29*, 291.
- [10] K. P. Schroder, J. Sauer, M. Leslie, C. R. A. Catlow, J. M. Thomas, *Chem. Phys. Lett.* **1992**, *188*, 320.
- [11] J. D. Gale, A. L. Rohl, in preparation.
- [12] A. Klamt, G. Schuurmann, *J. Chem. Soc. Perkin Trans. 2* **1993**, 799.
- [13] S. C. Parker, N. H. de Leeuw, S. E. Redfern, *Faraday Discuss.* **1999**, 381.
- [14] N. H. de Leeuw, F. M. Higgins, S. C. Parker, *J. Phys. Chem. B* **1999**, *103*, 1270.
- [15] S. D. Fleming, A. L. Rohl, S. C. Parker, G. M. Parkinson, *J. Phys. Chem. B* **2001**, *105*, 5099.
- [16] P. S. Singh, T. L. Dowling, J. N. Watson, J. W. White, *Phys. Chem. Chem. Phys.* **1999**, *1*, 4125.
- [17] R. T. Wilkin, H. L. Barnes, *Am. Mineral.* **2000**, *85*, 1329.
- [18] V. Nikolakis, E. Kokkoli, M. Tirrell, M. Tsapatsis, D. G. Vlachos, *Chem. Mater.* **2000**, *12*, 845.
- [19] C. S. Cundy, B. M. Lowe, D. M. Sinclair, *Faraday Discuss.* **1993**, 235.
- [20] J. N. Watson, L. E. Iton, R. I. Keir, J. C. Thomas, T. L. Dowling, J. W. White, *J. Phys. Chem. B* **1997**, *101*, 10094.
- [21] A. T. Davies, G. Sankar, C. R. A. Catlow, S. M. Clark, *J. Phys. Chem. B* **1997**, *101*, 10115.
- [22] S. Y. Yang, A. Navrotsky, *Microporous Mesoporous Mater.* **2002**, *52*, 93.
- [23] J. C. G. Pereira, C. R. A. Catlow, G. D. Price, *Chem. Commun.* **1998**, 1387.
- [24] M. J. Mora-Fonz, C. R. A. Catlow, D. W. Lewis, *Angew. Chem.* submitted **2004**.
- [25] A. Corma, F. Rey, M. J. Sabater, S. Valencia, Spanish patent number P200400662, Spain, **2004**.
- [26] A. Corma, F. Rey, J. Rius, M. J. Sabater, S. Valencia, *Nature* **2004**, *431*, 287.